Talanta 97 (2012) 16–22

Contents lists available at SciVerse ScienceDirect

Talanta

journal homepage: www.elsevier.com/locate/talanta

Ultrasonic assisted synthesis of adenosine triphosphate capped manganese-doped ZnS quantum dots for selective room temperature phosphorescence detection of arginine and methylated arginine in urine based on supramolecular Mg^{2+}–adenosine triphosphate–arginine ternary system

Hu-Bo Ren, Xiu-Ping Yan *

State Key Laboratory of Medicinal Chemical Biology, and Research Center for Analytical Sciences, College of Chemistry, Nankai University, Tianjin 300071, China

ARTICLE INFO

Article history:
Received 13 February 2012
Received in revised form
21 March 2012
Accepted 21 March 2012
Available online 3 May 2012

Keywords:
Ultrasonic assisted synthesis
Phosphorescence
Quantum dots
Adenosine triphosphate
Arginine

ABSTRACT

An ultrasonic assisted approach was developed for rapid synthesis of highly water soluble phosphorescent adenosine triphosphate (ATP)-capped Mn-doped ZnS QDs. The prepared ATP-capped Mn-doped ZnS QDs allow selective phosphorescent detection of arginine and methylated arginine based on the specific recognition nature of supramolecular Mg^{2+}–ATP–arginine ternary system in combination with the phosphorescence property of Mn-doped ZnS QDs. The developed QD based probe gives excellent selectivity and reproducibility (1.7% relative standard deviation for 11 replicate detections of 10 μM arginine) and low detection limit (3 s, 0.23 μM), and favors biological applications due to the effective elimination of interference from scattering light and autofluorescence.

1. Introduction

Arginine is an important component in biological systems, serving as a precursor for the synthesis of not only nitric oxide but also proteins, urea, proline, polyamines, glutamate, agmatine and creatine [1]. The main products of arginine methylation reactions are N^G, N^G-dimethylarginine (ADMA) and N^G, $N^{G'}$-dimethylarginine (SDMA) and these methylated arginine are liberated in the course of protein turnover and breakdown [1]. With the discovery of novel pathways for arginine catabolism and synthesis in humans, there is growing recognition that arginine is a conditionally essential amino acid in adult humans, particularly in cases of trauma or disease [2]. Owing to their biological importance, quite a few methods have been developed for the determination of arginine and methylated arginine in biological fluids based on high-performance liquid chromatography [3], capillary electrophoresis [4], enzymatic end-point analysis [5], thin-layer chromatography [6], amino acid analyzers [7], ion exchange paper chromatography [8], high-temperature paper chromatography [9], and voltammetry [10]. Even though, a simple, highly selective and sensitive, and instantaneous response method for the detection of arginine and methylated arginine is among the urgent and emerging challenges.

Photoluminescence spectrometry is the technique of choice for detecting arginine and methylated arginine owing to the apparent advantages of fluorescent probes over other methods in virtue of sensitivity and convenience. Miura et al. [11] reported the application of organic dyes as photoluminescence probe for highly specific detecting arginine. Quantum dots (QDs) offer unique advantages over organic dyes such as great photostability, high photoluminescence efficiency, size-dependent emission wavelengths, broad excitation and sharp emission profiles, thus QDs have been widely explored for bioanalysis [12–17]. However, to the best of our knowledge, no work on the utilization of functionalized QDs for detecting arginine and methylated arginine has been reported so far.

The supramolecular interactions of Mg^{2+} and arginine with adenosine-triphosphate (ATP) have been investigated to understand the precise function of arginine and Mg^{2+} in the specific cleavage mechanism of the ATP at the molecular level. ATP hydrolysis is catalyzed by arginine and Mg^{2+}, which is involved in the catalytic mechanism, acting as a binding site for ATP or as a cofactor. Selective non-enzymatic catalysis of ATP hydrolysis in complicated biological system based on Mg^{2+}–ATP–arginine ternary system have received great attentions [18–24].

* Corresponding author. Tel./fax: +86 22 23506075.
E-mail addresses: xpyan@nankai.edu.cn, xiupingyan@gmail.com (X.-P. Yan).

0039-9140/$ - see front matter © 2012 Elsevier B.V. All rights reserved.
http://dx.doi.org/10.1016/j.talanta.2012.03.055

Here we show ultrasonic assisted synthesis of ATP-capped Mn-doped ZnS QDs for rapid, selective and sensitive detection of arginine by taking the advantages of the outstanding optical properties of Mn-doped ZnS QDs and the Mg^{2+}–ATP–arginine ternary system for specific recognition of arginine. The ultrasonic approach was used for the synthesis of ATP-capped QDs because of its rapid, simple, low cost, and efficient merits [25]. Mn-doped ZnS QDs were used as photoluminescent probe due to their low toxicity and their long lifetime of phosphorescence which allowed an appropriate delay time to avoid interference from any background fluorescence emission and scattering light [26–28]. The choice of ATP as capping ligand in synthesis of functional QDs provided a powerful means of rationally controlling Mn-doped ZnS QDs properties. ATP could render Mn-doped ZnS QDs stable against aggregation and water-soluble, and retain the nucleotides structure needed to specially bind to its target [29]. The specific binding of ATP-capped Mn-doped ZnS QDs to arginine in the presence of Mg^{2+} led to highly selective quenching of the phosphorescence of the QDs, allowing selective detection of arginine with a detection limit of 0.23 μM.

2. Experimental section

2.1. Materials and chemicals

All chemicals used were at least analytical grade. Arginine, tyrosine, lysine, valine, serine, leucine, cystine, proline, aspartate, alanine, histidine, threonine, phenylalanine, methionine, glutamic acid, tryptophan, L-cysteine, glutathione and ATP disodium salt were purchased from Newprobe Biotechnology Co. Ltd. (Beijing, China). $Mg(NO_3)_2 \cdot 6H_2O$, $Zn(CH_3COO)_2 \cdot 2H_2O$, $Mn(CH_3COO)_2 \cdot 4H_2O$, and $Na_2S \cdot 9H_2O$ were purchased from Tianjing Guangfu Chemical Co. (Tianjing, China). ADMA and SDMA were obtained from Sigma (Steinheim, Germany). Citrulline (CIT) was obtained from Chinese Medicine Shanghai Chemical Reagent Supply Station (Shanghai, China). Ultrapure water (18.2 MΩ cm) obtained from a WaterPro water purification system (Labconco Corporation, Kansas City, MO, USA) was used throughout.

2.2. Apparatus

The microstructure and morphology of the QDs were characterized by high-resolution transmission electron microscopy (HRTEM) on a Philips Tecnai G2 F20 microscope (Philips, Holland) operating at a 200 kV accelerating voltage. The samples for HRTEM were obtained by drying sample droplets from water dispersion onto a 300-mesh Cu grid coated with a lacey carbon film. Fourier transform infrared (FT-IR) spectra (4000–400 cm^{-1}) in KBr were recorded on a Magna-560 spectrometer (Nicolet, Madison, WI). The X-ray diffraction (XRD) spectra were collected on a Rigaku D/max-2500 X-ray diffractometer (Rigaku, Japan) with Cu K_α radiation. The UV spectra were recorded on a UV-3600 spectrometer (Shimadzu, Japan). The decayed curves of phosphorescence emission at 595 nm excited by the N_2 laser at 337 nm were recorded on a PTI QM/TM/NIR system (Birmingham, NJ, USA). All nuclear magnetic resonance (NMR) experiments were carried out on a Bruker Avance 400 MHz spectrometer operating at 25 °C. The chemical shifts of ^{31}P NMR spectra in ppm were relative to an external reference of 85% H_3PO_4. In a typical experiment, 20% D_2O/H_2O was placed in a 5 mm NMR tube. For each sample, the probe was automatically locked, tuned, matched, and shimmed.

The ultrasonic assisted synthesis of ATP-capped Mn-Doped ZnS QDs was carried out on XiangHu Microwave-ultrasound reactor (XH-300 A, XiangHu Science and Technology Development Co. Ltd, Beijing, China). The phosphorescence measurements were performed on an F-4500 spectrofluorometer (Hitachi, Japan) equipped with a plotter unit and a quartz cell (1×1 cm^2) in the phosphorescence mode. The photomultiplier tube voltage was set at 950 V. The slit width was 10 nm and 20 nm for excitation and emission, respectively.

2.3. Ultrasonic assisted synthesis of ATP- capped Mn-doped ZnS QDs

The highly luminescent ATP-capped Mn-doped ZnS QDs were prepared in an aqueous solution at room temperature under ultrasonication. Typically, 5 mL of 0.04 M ATP, 5 mL of 0.1 M $Zn(CH_3COO)_2$ and 0.2 mL of 0.1 M $Mn(CH_3COO)_2$ were mixed with 40 mL ultrapure water in a 100 mL three-necked flask under ultrasonication at a power of 1000 W under argon for 7 min. 5 mL of 0.1 M $Na_2S \cdot 9H_2O$ was then added and the mixture was subjected ultrasonification at a power of 1000 W for 30 min to yield highly luminescent ATP-capped Mn-doped ZnS QDs. The obtained ATP-capped Mn-doped ZnS QDs was precipitated with ethanol, and separated by centrifuging at 10,000 rpm for 10 min. The final product was redissolved in ultrapure water, and diluted to appropriate concentration before detection. Uncapped Mn-doped ZnS QDs were synthesized using a similar procedure but without the addition of ATP.

2.4. Urine sample collection and pretreatment

Human urine samples were collected from healthy volunteers. The samples were subsequently centrifuged at 3000 rpm for 20 min to remove particulates. All samples were subjected to a 50-fold dilution before analysis and no other pretreatments were necessary.

2.5. Measurement procedures

To a 10 mL calibrated test tube an appropriate volume of 7 mg L^{-1} ATP-capped Mn-doped ZnS QDs solution, 0.1 mL of CH_3COOH–CH_3COONa buffer solution (0.1 M, pH 6.0), 100 μM $Mg(NO_3)_2 \cdot 6H_2O$ and a given concentration of arginine/methylated arginine standard solution or urine sample solution were sequentially added. The mixture was then diluted to volume with ultrapure water, mixed thoroughly, and incubated for 5 min. Finally, the phosphorescence measurements were performed on an F-4500 spectrofluorometer in phosphorescence mode with the excitation wavelength of 300 nm.

3. Results and discussion

3.1. Preparation and characterization of ATP-capped Mn-doped ZnS QDs

The ultrasonic assisted aqueous synthesis of ATP-capped Mn-doped ZnS QDs was carried out on the basis of the reaction of ATP, $Zn(CH_3COO)_2$, $Mn(CH_3COO)_2$ and Na_2S at room temperature. A period of 7 min was found sufficient to mix $Zn(CH_3COO)_2$, $Mn(CH_3COO)_2$ and ATP, and to ensure subsequence synthesis of highly luminescent ATP-capped Mn-doped ZnS QDs (Fig. S1 in the Supplementary Data). To show the merits of ultrasonic assisted synthesis of ATP-capped Mn-doped ZnS QDs, traditional method for synthesis of ATP-capped Mn-doped ZnS QDs based on a previous publication [30] was also used for comparison. A 2-h aging of the ATP-capped Mn-doped ZnS QDs was required to improve the phosphorescence intensity in the traditional method, whereas no such aging was necessary in our present ultrasonic assisted approach (Fig. S2 in the Supplementary Data). The present ultrasonic assisted approach not only provided a much faster synthesis (37 min *versus* 170 min), but also gave 2.3 times

higher phosphorescence intensity than the traditional method (Fig. S2 in the Supplementary Data).

The prepared ATP-capped Mn-doped ZnS QDs were characterized by XRD, FT-IR spectroscopy and HRTEM. The XRD pattern of the ATP-capped Mn-doped ZnS QDs exhibits a zinc blende with peaks for (111), (220), and (311) planes (Fig. 1A). The FT-IR spectra of the free ligand (ATP), ATP-capped Mn-doped ZnS QDs, and uncapped Mn-doped ZnS QDs were compared to confirm the coordination of the ATP on the surface of the QDs (Fig. 1B). ATP-capped Mn-doped ZnS QDs displayed a higher energy shift in the $-NH_2$ feature from 1713 cm^{-1} in the free ATP to 1650 cm^{-1}, suggesting the amine group on the adenine moiety was coordinated to the Mn-doped ZnS QDs surface [31,32]. The feature bands associated with the phosphate group (*ca.* 800–1300 cm^{-1}), the asymmetric stretching vibrations of the PO_2^- (*ca.* 1258 cm^{-1}), the out of phase symmetrical stretches (*ca.* 1104 cm^{-1}), and the P–O stretches of the main chain (*ca.* 971 cm^{-1}) were all broadened and slightly shifted in ATP-capped Mn-doped ZnS QDs, confirming the phosphate groups also coordinated to the surface of the QDs [33]. However, the bands at 1650, 1250 and 971 cm^{-1} disappeared in the FT-IR spectra of uncapped Mn–ZnS QDs. These results indicate the successful capping of ATP on the surface of the QDs, and the $-NH_2$, phosphate groups were involved in the interactions between ATP and the QDs. The HRTEM images reveal spherical shape of ATP-capped Mn-doped ZnS QDs with the diameters of 3–5 nm (Fig. 1C,D).

3.2. Consideration of supramolecular Mg^{2+}–ATP–arginine ternary system for QDs based phosphorescence sensing of arginine

The supramolecular interactions of Mg^{2+} and arginine with ATP have been investigated in complicated biological system [18–24]. In the Mg^{2+}–ATP–arginine ternary system, the binding interaction of Mg^{2+} with ATP involves not only N1 and N7 in the adenine ring but also phosphate groups of ATP. The binding forces are mainly cation (Mg^{2+})–π interaction and electrostatic interaction. Arginine is fully protonated under physiological conditions, and enables interaction with phosphate in ATP because of the strong basic nature of the guanidinium group. The role of arginine is to stabilize Mg^{2+}–ATP in the ternary system because the size and shape of arginine and ATP are compatible with a creation arrangement. Also, electrostatic interaction and coordination bonds are possibly involved in the interactions [18]. Such supramolecular Mg^{2+}–ATP–arginine ternary system gives us a hint to develop selective QDs based phosphorescence sensing of arginine in the presence of Mg^{2+}.

To take the advantages of the specific recognition of arginine based on the Mg^{2+}–ATP–arginine ternary system and the distinguished photoluminescence intrinsic of Mn-doped ZnS QDs, we designed and prepared ATP-capped Mn-doped ZnS QDs for sensing arginine in the presence of Mg^{2+} (Scheme 1). ATP not only renders Mn-doped ZnS QDs water-soluble and stable in aqueous solution against aggregation, but also retains the nucleotides structure needed to specifically bind to its target [29].

It is worth mentioning that the phosphorescence of ATP-capped Mn-doped ZnS QDs was quenched quickly upon addition of arginine in the presence of Mg^{2+}, and reached equilibrium within 5 min (Fig. 2). We ruled out the energy transfer from ATP-capped Mn-doped ZnS QDs to arginine in the presence of Mg^{2+} as the phosphorescence quenching mechanism because of no spectra overlap between the absorption spectra of arginine (and/or Mg^{2+}) and the phosphorescence emission spectra of ATP-capped Mn-doped ZnS QDs (Fig. 3A). The negligible variation in UV and resonance light scattering (RLS) spectra after adding Mg^{2+} and

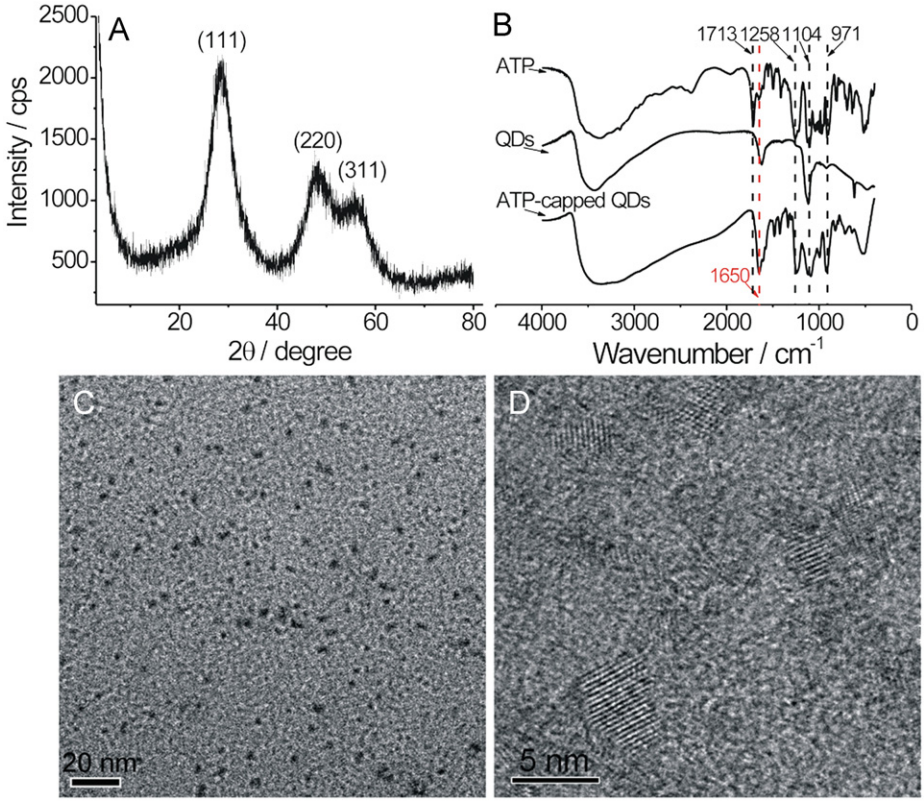

Fig. 1. (A) XRD pattern of the prepared ATP-capped Mn-doped ZnS QDs; (B) FT-IR spectra of ATP, uncapped Mn-doped ZnS QDs and ATP-capped Mn-doped ZnS QDs; (C) and (D) HRTEM images of the prepared ATP-capped Mn-doped ZnS QDs.

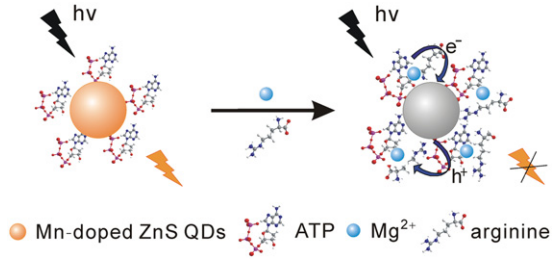

Scheme 1. Schematic illustration for the application of ATP-capped Mn-doped ZnS QDs for phosphorescence sensing arginine based on Mg^{2+}–ATP–arginine ternary system.

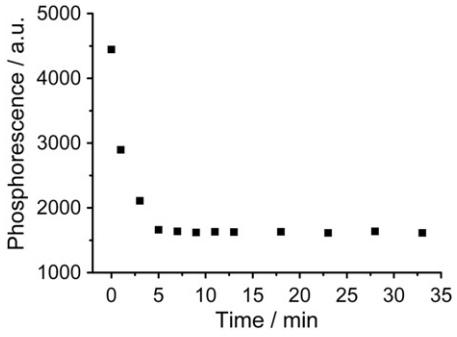

Fig. 2. Time-dependent phosphorescence intensity of ATP-capped Mn-doped ZnS QDs (6 mg L^{-1}) upon addition of Mg^{2+} (200 μM) and arginine (200 μM) in CH_3COOH–CH_3COONa buffer (1 mM, pH 6.0) at 595 nm.

arginine to the solution of ATP-capped Mn-doped ZnS QDs excluded the aggregation of the QDs in the presence of Mg^{2+} and arginine (Fig. 3A,B). In addition, the presence of arginine and Mg^{2+} led to little change of the emission decay behavior of ATP-capped Mn-doped ZnS QDs (Fig. 3(C); Table S1 in the Supplementary Data). Based on the above observations, we assumed that the arginine and Mg^{2+} occupied hole sites, and blocked the recombination process of electrons and holes, thereby decreasing the density of luminescent centers, and quenching the phosphorescence of ATP-capped Mn-doped ZnS QDs without affecting the decay kinetics radiative and nonradiative processes.

The phosphorescence quenching of ATP-capped Mn-doped ZnS QDs in the presence of arginine followed the Lineweaver–Burk equation (Eq. (1)) [34,35]

$$1/(P_0-P) = 1/P_0 + K_{LB}/(P_0 C_{Arginine}) \quad (1)$$

where P_0 and P are the phosphorescence intensity in the absence and presence of arginine, respectively, $C_{Arginine}$ is the concentration of arginine, K_{LB} is the static quenching constant [36–39]. The linear relationship between $(P_0-P)^{-1}$ and the concentration of arginine in the presence of 100 μM Mg^{2+} shows that the phosphorescence quenching in the present ternary system followed the static quenching (Fig. 4). The static quenching constant K_{LB} was found to be 16.7 from the slope of the Lineweaver–Burk plot.

^1H and ^{31}P NMR spectra were further used to reveal the interactions of ATP-capped Mn-doped ZnS QDs and arginine in the presence of Mg^{2+}. In the Mg^{2+}–ATP–arginine ternary system, the binding interaction of Mg^{2+} with ATP involves not only N1 and N7 in the adenine ring but also β- and γ-phosphate of ATP (Fig. 5A). The guanidinium group of arginine also interacts with β- and γ-phosphate of ATP [18–24]. The ^{31}P chemical shifts of ATP-capped Mn-doped ZnS QDs, ATP-capped Mn-doped ZnS QDs–Mg^{2+}, ATP-capped Mn-doped ZnS QDs–arginine, and ATP-capped Mn-doped ZnS QDs–Mg^{2+}–arginine (Fig. 5(B)–(E)) provide the information on the interaction between the phosphate chain of

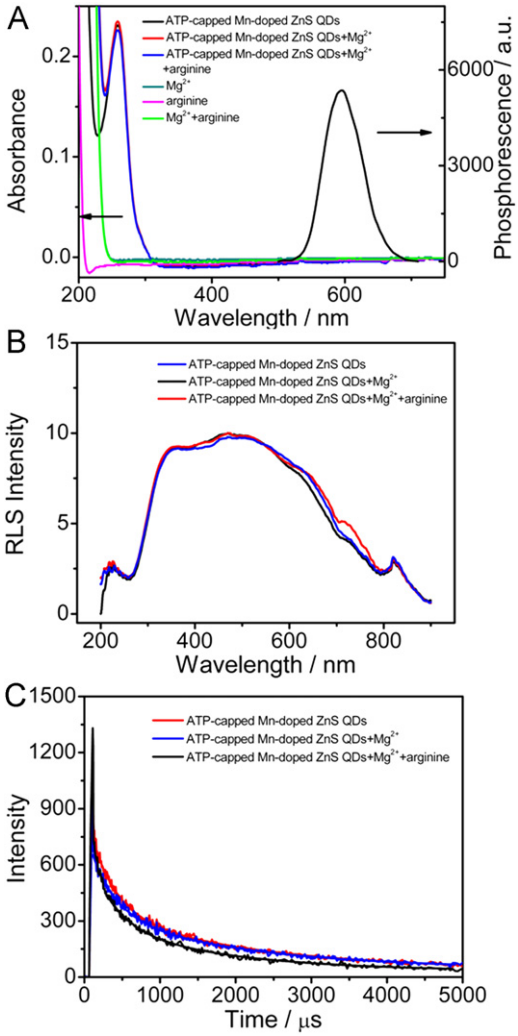

Fig. 3. (A) UV–vis spectra of Mg^{2+} (100 μM), arginine (100 μM), and ATP-capped Mn-doped ZnS QDs (7 mg L^{-1}) in the absence and presence of Mg^{2+} (100 μM), arginine (100 μM), and the phosphorescence emission spectra of ATP-capped Mn-doped ZnS QDs (7 mg L^{-1}); (B) RLS spectra of ATP-capped Mn-doped ZnS QDs (7 mg L^{-1}) in the absence and presence of Mg^{2+} (100 μM) and arginine (100 μM); (C) Decay curves of the phosphorescence emission of ATP-capped Mn-doped ZnS QDs (70 mg L^{-1}) alone or in the presence of Mg^{2+} (1 mM), arginine (1 mM). The three averaged scans of phosphorescence emission at 595 nm (300 channels) were recorded under excitation of a N_2 laser at 337 nm. All solution were prepared in 1 mM CH_3COOH–CH_3COONa buffer at pH 6.0.

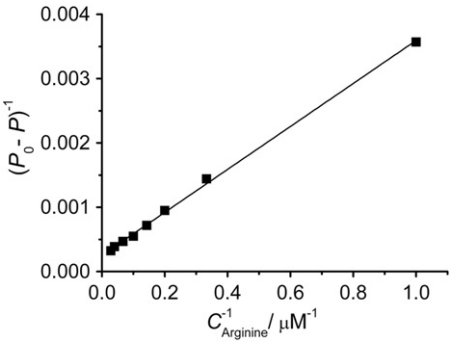

Fig. 4. Lineweaver–Burk plot for the interaction of ATP-capped Mn-doped ZnS QDs (7 mg L^{-1}), Mg^{2+} (100 μM) and arginine.

ATP-capped Mn-doped ZnS QDs, Mg^{2+} and arginine. It is clear that P_β and P_γ were involved in the binding interaction in the ternary system because the chemical shifts of P_β and P_γ exhibited

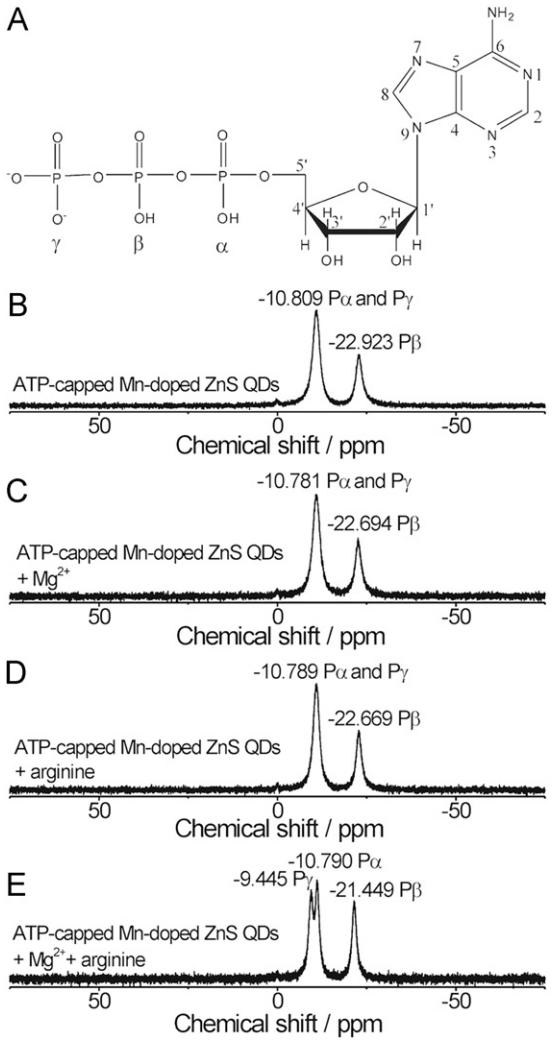

Fig. 5. (A) Structure of ATP; ^{31}P NMR spectra of ATP-capped Mn-doped ZnS QDs alone (2.8 g L^{-1}) (B), and in the presence of Mg^{2+} (70 mM) (C), arginine (70 mM) (D), and Mg^{2+} (70 mM) and arginine (70 mM) (E), respectively.

downfield shifts (Fig. 5B–E). The upfield shifts of H8 and H2 upon addition of Mg^{2+} and arginine to ATP-capped Mn-doped ZnS QDs resulted from the interaction at N7 and N1 of ATP (Fig. S3 in the Supplementary Data). ^{1}H NMR experiments indicate that Mg^{2+} and arginine promoted stacking of purine bases in the system. As a result, a significant difference between the binary (ATP-capped Mn-doped ZnS QDs and Mg^{2+}, ATP-capped Mn-doped ZnS QDs and arginine) and the ternary system (ATP-capped Mn-doped ZnS QDs, Mg^{2+} and arginine) in ^{1}H and ^{31}P NMR spectra, indicating that arginine is essential to the stabilization of the intermediate.

3.3. Factors affecting the sensitivity of the ATP-capped Mn-doped ZnS QDs for the phosphorescence detection of arginine

Fig. 2 shows the time-dependent phosphorescence quenching response of the ATP-capped Mn-doped ZnS QDs to arginine in the presence of Mg^{2+} in CH_3COOH–CH_3COONa buffer solution (1 mM, pH 6.0). The phosphorescence of the ATP-capped Mn-doped ZnS QDs was quenched by about 63% in 5 min after the addition of arginine, and remained unchanged with further increase of detection time, indicating that it was fast to reach equilibrium for the interaction among arginine, Mg^{2+} and ATP-capped Mn-doped ZnS QDs.

The phosphorescence quenching of the ATP-capped Mn-doped ZnS QDs was pH-dependent. The quenched phosphorescence intensity significantly increased as pH varied from 3 to 6, rapidly decreased from pH 6 to 7, and slightly changed with further increase of pH (Fig. 6A). The pH value of 6 was chosen for the further experiments due to the most quenching effect on the phosphorescence of ATP-capped Mn-doped ZnS QDs. It is possible that the pH effect is associated with the interaction of Mg^{2+} with the ATP-capped Mn-doped ZnS QDs due to the pH dependent ionization or protonation of ATP [18].

The phosphorescence quenching of the ATP-capped Mn-doped ZnS QDs also depended on the concentration of CH_3COOH–CH_3COONa buffer. The quenched phosphorescence intensity of the QDs decreased as the concentration of CH_3COOH–CH_3COONa buffer increased. To keep the QDs as stable as possible and to ensure sensitive determination of arginine, 1 mM of CH_3COOH–CH_3COONa buffer solution was used (Fig. 6B). The concentration of ATP-capped Mn-doped ZnS QDs influence the quenched phosphorescence intensity caused by arginine (Fig. 6C). 7 mg L^{-1} of ATP-capped Mn-doped ZnS QDs gave the highest sensitivity. The quenched phosphorescence of ATP-capped Mn-doped ZnS QDs varied with Mg^{2+} concentration (Fig. 6D). The quenched phosphorescence intensity of the QDs increased rapidly as the concentration of Mg^{2+} increased from 10 to 100 μM, and remained unchanged with further increase of the concentration of Mg^{2+}. Therefore, 100 μM of Mg^{2+} solution was used for the rest experiments.

3.4. Characteristic data of the ATP-capped Mn-doped ZnS QDs for the phosphorescence detection of arginine

Under the above optimal conditions, the phosphorescence intensity of the ATP-capped Mn-doped ZnS QDs gradually decreased as the concentration of arginine increased in the presence of Mg^{2+} (Fig. 7A). Statistical analysis of the quenched phosphorescence intensity *versus* the arginine concentration ($C_{Arginine}$) revealed two linear ranges for arginine sensing (Fig. 7B). The quenched phosphorescence intensity (ΔP) linearly increased with arginine concentration from 1 to 10 μM with a calibration function of $\Delta P = 171.3C_{Arginine} + 158.7$ ($R^2 = 0.992$), and from 10 to 35 μM with a calibration function of $\Delta P = 50C_{Arginine} + 1349.5$ ($R^2 = 0.997$). The phenomenon of two linear ranges for arginine sensing probably resulted from the integration of the Mg^{2+}–ATP–arginine ternary system and the hydrolysis of ATP catalyzed by Mg^{2+} and arginine. However, the exact reasons are still not clear at the present stage and need further investigation. The developed ATP-capped Mn-doped ZnS QDs gave the detection limit (LOD) (3 s) of 0.23 μM for arginine with the relative standard deviation of 1.7% for eleven replicate detections of 10 μM arginine.

3.5. Selectivity of the ATP-capped Mn-doped ZnS QDs for the phosphorescence detection of arginine

To demonstrate the selectivity of the ATP-capped Mn-doped ZnS QDs for the phosphorescence detection of arginine based on Mg^{2+}–ATP–arginine ternary system, the phosphorescence response of the ATP-capped Mn-doped ZnS QDs to arginine, methylated arginine (ADMA and SDMA), other 17 species of amino acids and glutathione were investigated (Fig. 8). Tyrosine, lysine, valine, serine, leucine, cystine, proline, aspartate, alanine, histidine, threonine, phenylalanine, methionine, glutarnate, tryptophan, citrulline, and cysteine were chosen since they are the most studied amino acids in previous QD-based amino acids probes. As shown in Fig. 8, other 17 species of amino acids and glutathione caused negligible phosphorescence response. In

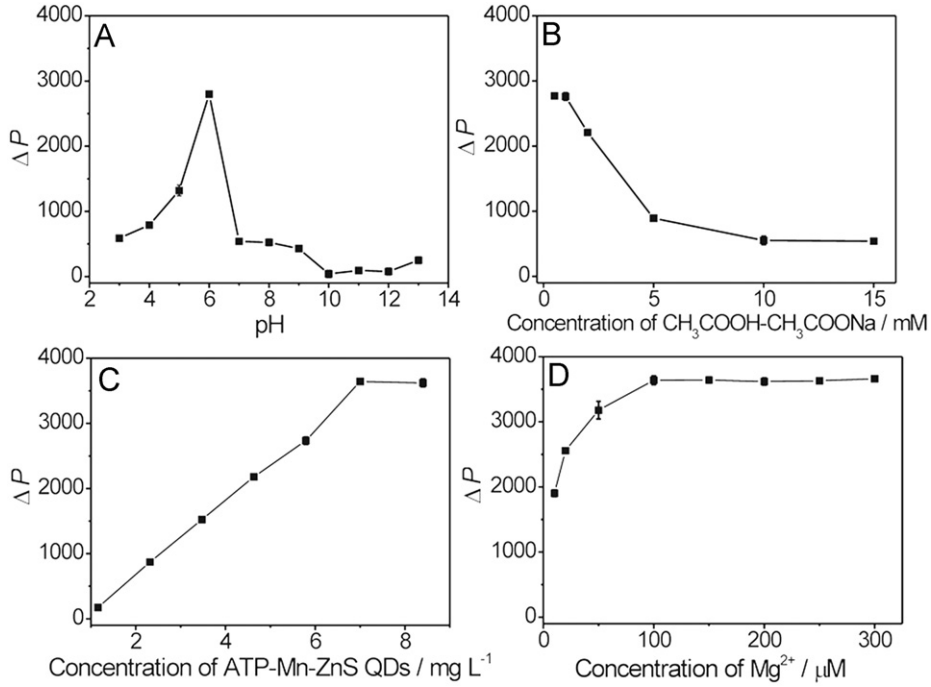

Fig. 6. Dependence of phosphorescence quenching of ATP-capped Mn-doped ZnS QDs caused by arginine (200 μM) on: (A) pH (6 mg L^{-1} ATP-capped Mn-doped ZnS QDs, 1 mM CH_3COOH–CH_3COONa buffer, 200 μM Mg^{2+}); (B) concentration of CH_3COOH–CH_3COONa buffer (6 mg L^{-1} ATP-capped Mn-doped ZnS QDs, pH 6.0, 200 μM Mg^{2+}); (C) concentration of ATP-capped Mn-doped ZnS QDs (1 mM CH_3COOH–CH_3COONa buffer, pH 6.0, 200 μM Mg^{2+}); (D) concentration of Mg^{2+} (7 mg L^{-1} ATP-capped Mn-doped ZnS QDs, 1 mM CH_3COOH–CH_3COONa buffer, pH 6.0). $\Delta P = P_0 - P$ denotes the quenched phosphorescence intensity of ATP-capped Mn-doped ZnS QDs.

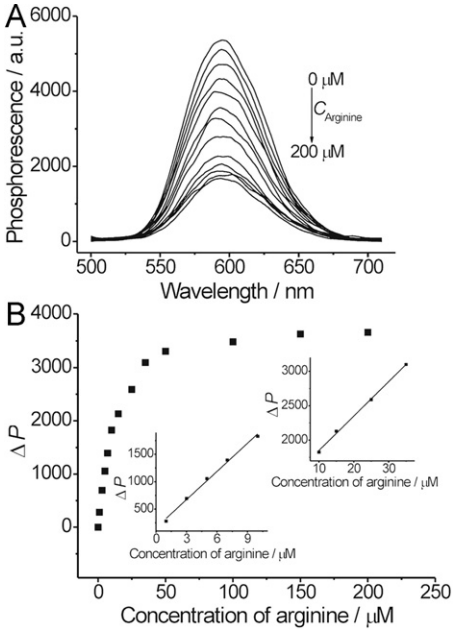

Fig. 7. (A) Effect of the concentration of arginine on the phosphorescence spectra of the ATP-capped Mn-doped ZnS QDs in the presence of Mg^{2+}; (B) Plots of the quenched phosphorescence intensity as a function of arginine concentration, showing two linear ranges. Buffer, 1 mM CH_3COOH–CH_3COONa (pH 6.0); ATP-capped Mn-doped ZnS QDs, 7 mg L^{-1}; Mg^{2+}, 100 μM. ΔP denotes the quenched phosphorescence intensity of ATP-capped Mn-doped ZnS QDs.

contrast, only arginine and methylated arginine resulted in significant phosphorescence quenching of the ATP-capped Mn-doped ZnS QDs. The above results show excellent selectivity of the developed probe for arginine and methylated arginine with same sensitivity (Fig. 8; Fig. S4 in the Supplementary Data).

The ATP-capped Mn-doped ZnS QDs also gave excellent selectivity for detecting arginine in the presence of main relevant metal ions, biomolecules and other amino acids in urine samples (Table S2 in the Supplementary Data). Quenching of the phosphorescence emission due to the addition of arginine at 3 μM was unaffected by 1 mM Na^+, 4 mM K^+, 800 μM Ca^{2+}, 500 μM Mg^{2+}, 10 μM Zn^{2+}, 8 μM Mn^{2+}, 2 mM glucose, 200 μM urea, 30 μM uric acid, 200 μM ascorbic acid, 100 μM citric acid, 50 mg L^{-1} HSA, 30 μM tyrosine, 50 μM lysine, 50 μM valine, 50 μM serine, 50 μM leucine, 30 μM cystine, 50 μM proline, 50 μM aspartate, 50 μM alanine, 30 μM histidine, 50 μM threonine, 50 μM phenylalanine, 50 μM methionine, 30 μM glutamic acid, 30 μM tryptophan, 6 μM L-cysteine and 5 μM glutathione. The interference from L-cysteine and glutathione likely resulted from the strong affinity of the thiol groups on L-cysteine and glutathione to the QDs surface. As the concentration of L-cysteine and glutathione in human urine samples are about 85 and 23 μM, respectively [40], no such interference was observed when 50-fold dilution of urine samples were performed before analysis (Table 1). For the analysis of samples with high concentration of the L-cysteine and glutathione, the interferences from L-cysteine and glutathione can be eliminated or minimized by using thiol-blocking reagents, such as N-ethylmaleimide.

3.6. Determination of arginine and methylated arginine in urine samples

The developed biosensor was further applied to the phosphorescence determination of arginine and methylated arginine in four urine samples. No phosphorescence background from urine was observed although the fluorescence background from urine was significant (Fig. S4 in the Supplementary Data). A 50-fold dilution of urine was found sufficient to obtain a quantitative recovery (94–100%) of spiked arginine and to use a simple aqueous standard solution for the accurate quantification of arginine and methylated arginine (Table 1, Fig. S5 in the Supplementary Data). The results generated by this method correspond well with previously published data [41].

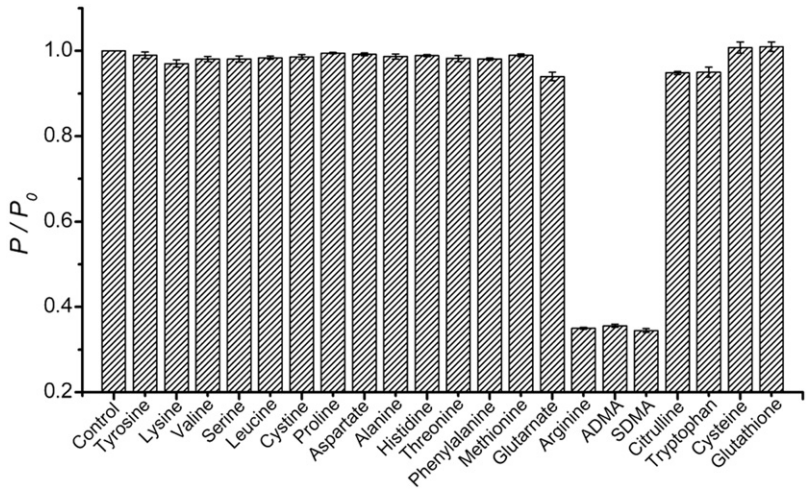

Fig. 8. Response of ATP-capped Mn-doped ZnS QDs (7 mg L^{-1}) in the presence of Mg^{2+} (100 μM) to arginine (100 μM), ADMA (100 μM), SDMA (100 μM), other amino acids (100 μM) and glutathione (100 μM) in CH_3COOH–CH_3COONa buffer (1 mM, pH 6.0). P and P_0 denote the phosphorescence intensity of ATP-capped Mn-doped ZnS QDs in the presence and absence of arginine, respectively.

Table 1
Analytical results for arginine and methylated arginine in human urine samples.

Sample	Concentration found (mean ± s, $n=3$) (μM) [a]	Recovery (%) [b]
Urine 1	134 ± 6	94.4 ± 3
Urine 2	148 ± 17	97.8 ± 4
Urine 3	107 ± 9	95.8 ± 3
Urine 4	144 ± 28	96.1 ± 5

[a] The found concentrations were already adjusted for the dilution factor, thereby representing the total concentration of arginine and methylated arginine in the original urine samples.
[b] For spiking 150 μM arginine in original urine samples.

4. Conclusions

In summary, we have reported an ultrasonic assisted synthesis of ATP-capped Mn-doped ZnS QDs for selective detection of arginine and methylated arginine based on the specific recognition nature of Mg^{2+}–ATP–arginine ternary system in combination with the phosphorescence property of Mn-doped ZnS QDs. The developed probe gives excellent selectivity and reproducibility, and low detection limit. The developed phosphorescence probe favors biological applications since the interference from scattering light and autofluorescence is effectively eliminated.

Acknowledgments

This work was supported by the National Basic Research Program of China (No. 2011CB707703), the National Natural Science Foundation of China (No. 20935001), and the Tianjin Natural Science Foundation (No. 10JCZDJC16300).

Appendix A. Supporting information

Supplementary data associated with this article can be found in the online version at http://dx.doi.org/10.1016/j.talanta.2012.03.055.

References

[1] G. Wu, S.M. Morris, Biochem. J. 336 (1998) 1–17.
[2] A. Barbul, J. Parenter. Enteral. Nutr. 10 (1986) 227–238.
[3] V. Gopalakrishnan, P.J. Burton, T.F. Blaschke, Anal. Chem. 68 (1996) 3520–3523.
[4] D.L. Olson, M.E. Lacey, A.G. Webb, J.V. Sweedler, Anal. Chem. 71 (1999) 3070–3076.
[5] R.M. de Orduña, J. Agric. Food Chem. 49 (2001) 549–552.
[6] S. Bahl, S. Naqvi, T.A. Venkitasubramanian, J. Agric. Food Chem. 24 (1976) 56–59.
[7] A. Bastone, L. Diomede, R. Parini, F. Carnevale, M. Salmona, Anal. Biochem. 191 (1990) 384–389.
[8] H.R. Roberts, M.G. Kolor, Anal. Chem. 31 (1959) 565–566.
[9] S.M. Sibalić, N.V. Radej, Anal. Chem. 33 (1961) 1223–1224.
[10] F.G. Bánicá, D. Guziejewski, S. Skrzypek, W. Ciesielski, D. Kaźmierczak, Electroanalysis 21 (2009) 1711–1718.
[11] T. Miura, M. Kashiwamura, M. Kimura, Anal. Biochem. 139 (1984) 432–437.
[12] M.J. Ruedas-Rama, E.A.H. Hall, Anal. Chem. 80 (2008) 8260–8268.
[13] W.C.W. Chan, S. Nie, Science 281 (1998) 2016–2018.
[14] M. Bruchez, M. Moronne, P. Gin, S. Weiss, A.P. Alivisatos, Science 281 (1998) 2013–2016.
[15] W.C.W. Chan, D.J. Maxwell, X. Gao, R.E. Bailey, M. Han, S. Nie, Anal. Biotechnol. 13 (2002) 40–46.
[16] X. Michalet, F.F. Pinaud, L.A. Bentolila, J.M. Tsay, S. Doose, J.J. Li, G. Sundaresan, A.M. Wu, S.S. Gambhir, S. Weiss, Science 307 (2005) 538–544.
[17] I.L. Medintz, H.T. Uyeda, E. Goldman, H. Mattoussi, Nat. Mater. 4 (2005) 435–446.
[18] Y.Q. Ma, G.X. Lu, Dalton Trans. (2008) 1081–1086.
[19] M. Fokkens, T. Schrader, F.G. Klärner, J. Am. Chem. Soc. 127 (2005) 14415–14421.
[20] M.F. Bush, J.T. O'Brien, J.S. Prell, R.J. Saykally, E.R. Williams, J. Am. Chem. Soc. 129 (2007) 1612–1622.
[21] A.S. Woods, S. Ferré, J. Proteome Res. 4 (2005) 1397–1402.
[22] A.S. Woods, J. Proteome Res. 3 (2004) 478–484.
[23] M.J. Rashkin, R.M. Hughes, N.T. Calloway, M.L. Waters, J. Am. Chem. Soc. 126 (2004) 13320–13325.
[24] R.M. Hughes, M.L. Waters, J. Am. Chem. Soc. 128 (2006) 13586–13591.
[25] J.L. Luche, C. Bianchi, Plenum Press, New York, 1998, pp. 91.
[26] H.F. Wang, Y. He, T.R. Ji, X.P. Yan, Anal. Chem. 81 (2009) 1615–1621.
[27] Y. He, H.-F. Wang, X.-P. Yan, Anal. Chem. 80 (2008) 3832–3837.
[28] H.-B. Ren, B.-Y. Wu, J.-T. Chen, X.-P. Yan, Anal. Chem. 83 (2011) 8239–8244.
[29] J.H. Choi, K.H. Chen, M.S. Strano, J. Am. Chem. Soc. 128 (2006) 15584–15585.
[30] J.Q. Zhuang, X.D. Zhang, G. Wang, D.M. Li, W.S. Yang, T.J. Li, J. Mater. Chem. 13 (2003) 1853–1857.
[31] M. Green, D. Smyth-Boyle, J. Harries, R. Taylor, Chem. Commun. (2005) 4830–4832.
[32] H. Sigel, Inorg. Chim. Acta 198–200 (1992) 1–11.
[33] M. Green, R. Taylor, G. Wakefield, J. Mater. Chem. 13 (2003) 1859–1861.
[34] K. Sauer, H. Scheer, P. Sauer, Photochem. Photobiol. 46 (1987) 427–440.
[35] J.R. Lakowicz, G. Weber, Biochemistry 12 (1973) 4161–4170.
[36] R.M. Jones, T.S. Bergstedt, D.W. McBranch, D.G. Whitten, J. Am. Chem. Soc. 123 (2001) 6726–6727.
[37] C.B. Murphy, Y. Zhang, T. Troxler, V. Ferry, J.J. Martin, W.E. Jones, J. Phys. Chem. B 108 (2004) 1537–1543.
[38] M.S. Baptista, G.L. Indig, J. Phys. Chem. B 102 (1998) 4678–4688.
[39] J.R. Lakowicz, Principle of Fluorescence Spectroscopy, 2nd ed., Plenum Press, New York, 1999, pp. 237–259.
[40] Y. Zhang, Y. Li, X.-P. Yan, Anal. Chem. 81 (2009) 5001–5007.
[41] J.M. Lobenhoffer, S.M. Bode-Böger, J. Chromatogr. B 798 (2003) 231–239.